

A mechanism for elliptic-like bursting and synchronization of bursts in a map-based neuron network

Hongjun Cao · Miguel A. F. Sanjuán

Received: 29 April 2008 / Revised: 4 July 2008 / Accepted: 11 July 2008 / Published online: 31 July 2008
© Marta Olivetti Belardinelli and Springer-Verlag 2008

Abstract A system consisting of two Rulkov map-based neurons coupled through reciprocal electrical synapses as a simple phenomenological example is discussed. When the electrical coupling is excitatory, the *square-wave* bursting can be well predicted by the bifurcation analysis of a comparatively simple low-dimensional subsystem embedded in the invariant manifold. While, when the synapses are inhibitory due to the artificial electrical coupling, a fast–slow analysis is carried out by treating the two slow variables as two different bifurcation parameters. The main result of this paper is to present a mechanism for the occurrence of a kind of special *elliptic* bursting. The mechanism for this kind of *elliptic-like bursting* is due to the interaction between two chaotic oscillations with different amplitudes. Moreover, the generation of antiphase synchronization of networks lies in the different switching orders between two pairs of different chaotic oscillations corresponding to the first neuron and the second neuron, respectively.

Keywords Map neurons · Bursting · Synchronization

Introduction

Map-based neuron models and map-based neuron networks (Gerstner and Kistler 1999; Nozawa 1992; Chialvo 1995; Rulkov et al. 2004; Rulkov 2001; de Vries 2001; Tanaka et al. 2006; Izhikevich 2007; Ibarz et al. 2007b), as a simplification of ordinary differential equations (ODE), have received much attention over the past years, especially when the collective behavior of large-scale networks of neurons is involved.

However, there are still some unclear problems, especially in the context of the analysis of the fast–slow dynamics corresponding to the fast subsystem of map-based models. For example, a very common method to study the dynamics of neuron networks consists of decomposing the fast and the slow subsystems, independently on being modeled as an ODE-based system or as a map-based system. As Rinzel (1987), Sherman (1996), Rulkov (2001, 2004), Shilnikov and Rulkov (2004), de Vries (2001), Izhikevich (2000) and many other researchers (Tanaka et al. 2006; Ibarz et al. 2007b; Casado 2003; Casado et al. 2004; Cao et al. 2007; Ibarz et al. 2007c; Ibarz et al. 2007a) have done before, slow variables are usually treated as a single bifurcation parameter in the fast subsystem. By doing so, the fast subsystem can be reduced into a much simpler low-dimensional system. Much progress has been made by using this kind of reduction techniques to predict the mechanism for bursting when some neuron networks are considered.

It is well known that there exist multiple slow variables besides the fast variables in the real neuron models (Izhikevich 2007). These slow variables are responsible for the transitions between the fast variables. Much attention has been paid on treating different slow variables as different bifurcation parameters in ODE-based neuron networks (Best et al. 2005). Nevertheless, less attention has been paid on

H. Cao
Department of Mathematics, School of Science,
Beijing Jiaotong University, Beijing 100044,
People's Republic of China
e-mail: hjcao@bjtu.edu.cn

H. Cao · M. A. F. Sanjuán (✉)
Nonlinear Dynamics and Chaos Group,
Departamento de Física, Universidad Rey Juan Carlos,
Tulipán s/n, 28933 Móstoles, Madrid, Spain
e-mail: miguel.sanjuan@urjc.es

treating slow variables as different bifurcation parameters in the fast–slow analysis for the fast subsystem of map-based neuron networks. Therefore, it is natural to wonder whether these slow variables of map-based neuron models can only be treated as a single bifurcation parameter.

Here, we take two identical Rulkov neurons (Rulkov et al. 2004) coupled by excitatory or inhibitory electrical synapses as a simple phenomenological example. The main goal of this paper is to show that even in this ensemble of two identical neurons, their two slow variables are unequal in most cases. It seems to be much more reasonable and predictable to use two different bifurcation parameters rather than to use only one, when bifurcation theory and geometric singular perturbation theory are applied.

Most spiking neurons can produce bursting phenomena if a current is stimulated so that the current slowly drives the neuron above and below the firing threshold. Such a current could be injected via an electrode or generated by the synaptic input. Neuronal spiking and bursting can play important roles in communication between neurons. In particular, bursting neurons are important for motor pattern generation and synchronization (Izhikevich 2007).

The numerical simulations at first show that there exist two types of bursting. One is the *square-wave* bursting resulting from a periodic transition between the silent phase corresponding to a steady state and the active phase corresponding to a chaotic oscillation. The mechanism for *square-wave* bursting is mainly due to bistability. And the other one is the *elliptic-like* bursting, which is characterized by an abrupt periodic switching between a small amplitude chaotic oscillation corresponding to the silent phase and a large amplitude chaotic oscillation corresponding to the active phase. In this case, there is no longer bistability in the fast subsystem. It is hard to explain and predict the occurrence of *elliptic-like* bursting if only a slow variable as a unique bifurcation is concerned. In addition, there exist many kinds of regular cooperative behaviors such as in-phase and antiphase synchronizations of bursts. Although the antiphase synchronization of bursts is made artificially under the effect of inhibitory electrical synapses, this is reasonable because this is motivated by an experimental result shown in Elson et al. (1998). In what we are really interested here is the mechanism of the generation and synchronization of bursts, since to the best of our knowledge, it does not seem to be fully well understood.

Second, we will investigate under what conditions, the two slow variables of Rulkov map-based networks assume equal or unequal values at any given time. We have found that corresponding to moderate excitatory or inhibitory electrical coupling strength, the two slow variables are usually unequal.

One of our main results demonstrates that when the excitatory electrical coupling is applied, there coexist

multiple stable branches of on-diagonal and off-diagonal fixed points of the fast subsystem. The key to predict the bursting and synchronization lies in the dynamical behaviors occurring on the invariant manifold. Due to the existence of an invariant manifold, much more complicated systems can be reduced into a comparatively simple low-dimensional subsystem by embedding them into the invariant manifold. The multiple stable branches of off-diagonal fixed points are only helpful in shaping the *square-wave* bursting, and besides that they have no other essential consequences for the prediction of the *square-wave* bursting.

The main novelty of this paper is to propose a mechanism for the occurrence of *elliptic-like* bursting when the electrical coupling is inhibitory. In this case, the fast subsystem includes two different slow variables no matter how small the coupling strength is. In this case, there coexist still two chaotic attractors. The *elliptic-like* bursting oscillation is due to the interaction between two chaotic oscillations with different amplitudes. Moreover, the generation of antiphase synchronization of networks lies in the different switching orders between two pairs of different chaotic oscillations of the first neuron and the second neuron. The mechanism is in agreement with experimental studies where two coupled neurons are coupled by an artificial dynamical current clamp device (Elson et al. 1998).

The layout of this paper is as follows. In “[Description of the coupled map-based neuron system](#)”, we give a description and its wave forms of two identical Rulkov map-based neurons coupled by excitatory or inhibitory electrical synapses, respectively. Corresponding to two kinds of different synaptic couplings, the bifurcation phenomena are examined by using one and two different bifurcation parameters of the fast subsystem in “[Excitatory electrical coupling](#)” and “[Inhibitory electrical coupling](#)”. Finally, we sum up our results with some comments in “[Conclusion and discussion](#)”.

Description of the coupled map-based neuron system

We consider here a simple neuron network composed of two identical Rulkov map-based neurons (Rulkov 2001) coupled through electrical or gap-junctional coupling

$$\begin{aligned}x_{n+1,1} &= \frac{\alpha}{1+x_{n,1}^2} + y_{n,1} + \varepsilon(x_{n,2} - x_{n,1}), \\y_{n+1,1} &= y_{n,1} - \eta(x_{n,1} - \sigma), \\x_{n+1,2} &= \frac{\alpha}{1+x_{n,2}^2} + y_{n,2} + \varepsilon(x_{n,1} - x_{n,2}), \\y_{n+1,2} &= y_{n,2} - \eta(x_{n,2} - \sigma),\end{aligned}\tag{1}$$

where α , ε , η , and σ are parameters. When η is very small, then the evolution of $y_{n,i}$ ($i = 1, 2$) is much slower than

that of $x_{n,i}$ ($i = 1, 2$). Thus, we refer to $x_{n,i}$ as the fast variables and $y_{n,i}$ as the slow variables, and the parameter ε denotes the electrical synaptic coupling strength. The full system of Eqs. (1) can be divided into the two following subsystems:

$$\begin{aligned} x_{n+1,1} &= \frac{\alpha}{1+x_{n,1}^2} + y_{n,1} + \varepsilon(x_{n,2} - x_{n,1}), \\ x_{n+1,2} &= \frac{\alpha}{1+x_{n,2}^2} + y_{n,2} + \varepsilon(x_{n,1} - x_{n,2}), \end{aligned} \tag{2}$$

and

$$\begin{aligned} y_{n+1,1} &= y_{n,1} - \eta(x_{n,1} - \sigma), \\ y_{n+1,2} &= y_{n,2} - \eta(x_{n,2} - \sigma). \end{aligned} \tag{3}$$

For convenience we call Eqs. (2) the fast subsystem, and Eqs. (3) the slow subsystem.

The detailed dynamics of the Rulkov map-based network before and after coupling through the mean field has been analyzed by Rulkov (2001) and de Vries (2001) by means of bifurcation theory and geometric singular perturbation theory. The two slow variables $y_{n,1}$ and $y_{n,2}$ are treated as a single bifurcation parameter γ in those works.

Therefore, the behavior of a single neuron can be well predicted by studying the one-dimensional fast subsystem $x_{n+1} = \alpha/(1+x_n^2) + \gamma$ (Rulkov 2001). Also, for a population of two identical neurons coupled by the mean field, bursting as an emergent phenomenon can also be approximately predicted by the dynamics of the other one-dimensional fast subsystem $x_{n+1} = \alpha/(1+x_n^2) + \gamma + \varepsilon x_n$ (Rulkov 2001; de Vries 2001). Their studies demonstrate that there are two key ingredients for bursting: (1) one is the bistability, which can be defined by a saddle-node bifurcation γ_{sn} and an external crisis bifurcation γ_{ec} . When $\gamma_{ec} < \gamma < \gamma_{sn}$, there coexist active and silent phases. During the silent phase the state of the neuron runs η -close to the stable branch of the curve of fixed points, while in the active phase, the state of the neuron exhibits rapid chaotic oscillations; (2) the other one is the nullcline $x_{n,1} = \sigma$. When $x_{n,1} = \sigma$, the slow variables $y_{n,i}$ do not change; when $x_{n,1} > \sigma$, the slow variables $y_{n,i}$ are decreasing; when $x_{n,1} < \sigma$, the slow variables $y_{n,i}$ are increasing.

If the electrical coupling strength ε is positive or negative, corresponding to excitatory or inhibitory couplings, then the wave forms of the full system, Eqs. (1), are shown

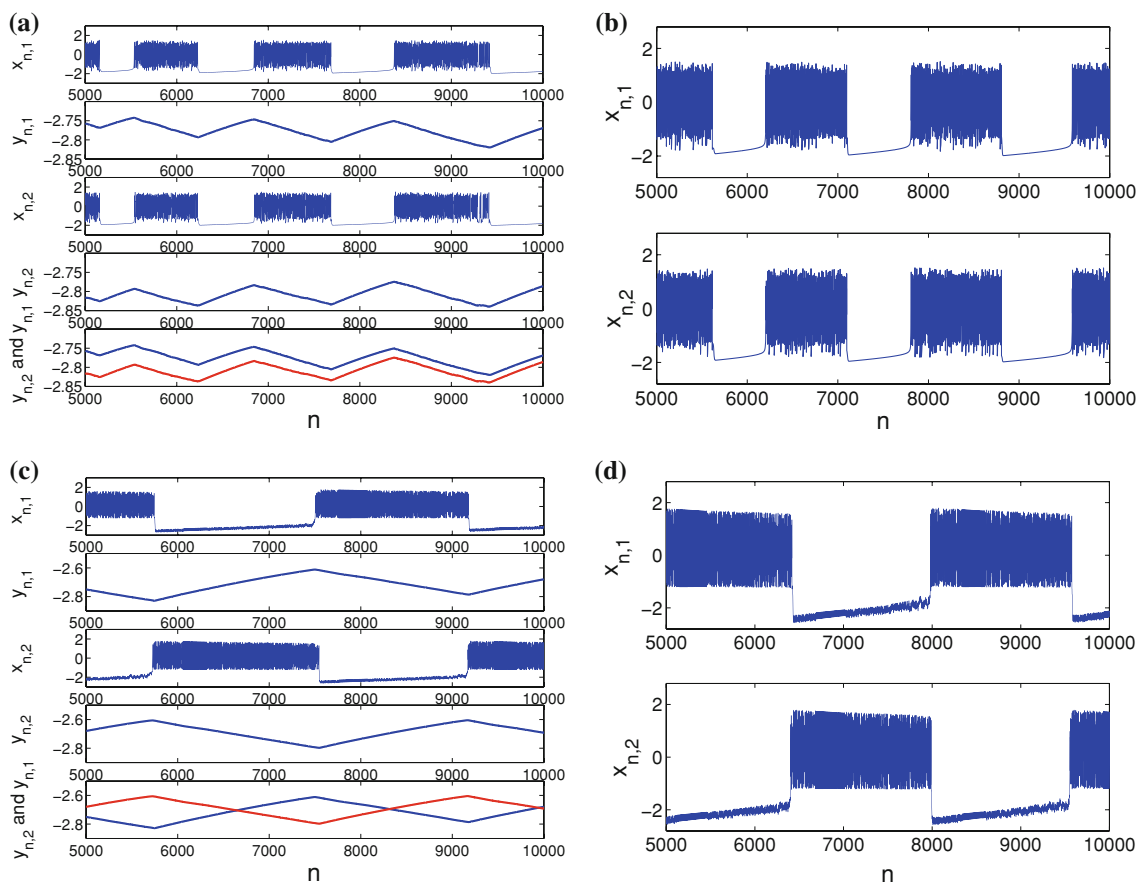


Fig. 1 Wave forms of Eqs. (1) coupled by the excitatory or inhibitory electrical synapses, respectively. **a** $\varepsilon = 0.1$; **b** a blow-up for $x_{n,1}$ and $x_{n,2}$ versus n of **a**; **c** $\varepsilon = -0.1$; **d** a blow-up for $x_{n,1}$ and $x_{n,2}$ versus n of **c**

in Fig. 1. We set the following parameters all throughout the paper to be $\alpha = 4.15$, $\nu = -2.5$, $\eta = 0.0001$, and particularly, the value of the nullcline is fixed at $\sigma = -1$.

A few typical wave forms of Eqs. (1) are shown in Fig. 1, and note that there exist two kinds of different synchronized patterns and two types of bursting oscillations. When the coupling is excitatory ($\varepsilon = 0.1$), the wave forms are in the state of in-phase synchronization, see Fig. 1a. However when the coupling is inhibitory ($\varepsilon = -0.1$), the wave forms are in the state of antiphase synchronization, see Fig. 1c. In addition, Fig. 1a display a type of *square-wave* bursting. This type of bursting oscillation is characterized by a periodic switching between the silent phase and the active phase of repetitive firings. Figure 1b shows a blow-up of the two fast variables $x_{n,i}$ ($i = 1,2$) versus n shown in Fig. 1a, in which the fast variables sit on a curve of fixed points during the silent phase. Afterwards, the fast variables go to a chaotic oscillation during the active phase. Figure 1c show a type of *elliptic-like* bursting, in which a kind of particular bursting occurs between the silent phase with a small amplitude oscillation and the active phase with a large amplitude oscillation. In contrast to the above case in the *square-wave* bursting, Fig. 1d provides a blow-up of the two fast variables $x_{n,i}$ versus n shown in Fig. 1c, where during the silent phase in the *elliptic-like* bursting, the fast variables sit on a small chaotic attractor with small amplitudes, and subsequently the fast variables move to the other chaotic attractor with comparative large amplitudes.

It is obvious to observe that from Fig. 1a and c, the two slow variables $y_{n,1}$ and $y_{n,2}$ are unequal. In addition, the difference between the two slow variables $y_{n,1}$ and $y_{n,2}$ will increase as the absolute value of the coupling strength ε increases. So, how the two slow variables make any difference in the case that they are treated as two different bifurcation parameters or in the case that there is only one?

Excitatory electrical coupling

In this section, the electrical coupling strength ε is supposed to be positive, so we have an excitatory electrical coupling. In this situation we have two different possibilities. When both slow variables are equal, we have a single bifurcation parameter and when they are unequal we have two bifurcation parameters.

$$y_{n,1} = y_{n,2} = \gamma$$

When ε is a small enough parameter, the two slow variables of Eqs. (1) are approximately equal. Consequently, the two slow variables $y_{n,1}$ and $y_{n,2}$ might be treated as a

single bifurcation parameter γ , and then the corresponding fast subsystem becomes:

$$\begin{aligned} x_{n+1,1} &= \frac{\alpha}{1+x_{n,1}^2} + \gamma + \varepsilon(x_{n,2} - x_{n,1}), \\ x_{n+1,2} &= \frac{\alpha}{1+x_{n,2}^2} + \gamma + \varepsilon(x_{n,1} - x_{n,2}). \end{aligned} \quad (4)$$

When $\varepsilon = 0.1$, the corresponding curves of fixed points of Eqs. (4) are presented in the $(\gamma, x_{n,1})$ plane. As shown in Fig. 2a, there coexist three S-shaped curves of fixed points which are S_1 , S_2 , and S_3 . In particular, the points on S_1 correspond to the on-diagonal fixed points satisfying the condition $x_{n,1} = x_{n,2}$, while the points on S_2 and S_3 correspond to the off-diagonal fixed points satisfying the condition $x_{n,1} \neq x_{n,2}$. Here, the solid blue points correspond to stable fixed points, and the red dashed points correspond to the unstable fixed points. The square stands for a Hopf bifurcation, and the triangle denotes a saddle-node bifurcation. There coexist multiple stable branches of fixed points of Eqs. (4) on the three S-shaped curves, for example, on S_1 , there coexist S_{11} , S_{12} , and S_{13} corresponding to on-diagonal fixed points, on S_2 and S_3 , there coexist S_{21} and S_{31} corresponding to off-diagonal fixed points, respectively. The lower left part of Fig. 2a can be seen clearly by observing a magnified version shown in Fig. 2b.

We are interested in multiple stable branches of off-diagonal fixed points of Eqs. (4). This is because the stable branches help us to know the silent phase of bursting. So in the following part of this section, the main goal is to analyze how the off-diagonal fixed points affect the generation of bursting.

By numerical simulations, three different bifurcation diagrams are shown in Fig. 2c–e, starting from different initial points situated on different stable branches of fixed points of Eqs. (4), respectively. Figure 2c shows the bifurcation diagram starting from an on-diagonal initial point on S_{12} , while Fig. 2d–e shows the bifurcation diagrams when the initial points are chosen from the off-diagonal fixed points on the stable branches S_{31} , and S_{21} , respectively. Note that when the bifurcation parameter γ reaches the leftmost external crisis bifurcation, corresponding to different initial conditions shown in Fig. 2c–e, the iterates of Eqs. (4) drop suddenly down onto the same bottom stable branch S_{11} , which corresponds to on-diagonal fixed points of Eqs. (4). That is to say, corresponding to three different initial conditions, when the bifurcation parameter γ reaches the rightmost external crisis bifurcation, all three types of iterates drop suddenly down onto the same bottom stable branch on S_{11} . Therefore, we refer to the bottom stable branch on S_{11} as the invariant manifold. The subsequent iterates are almost similar as we see from Fig. 2c–e. There exist some minor differences between Fig. 2c and d, e, which depends on the different initial

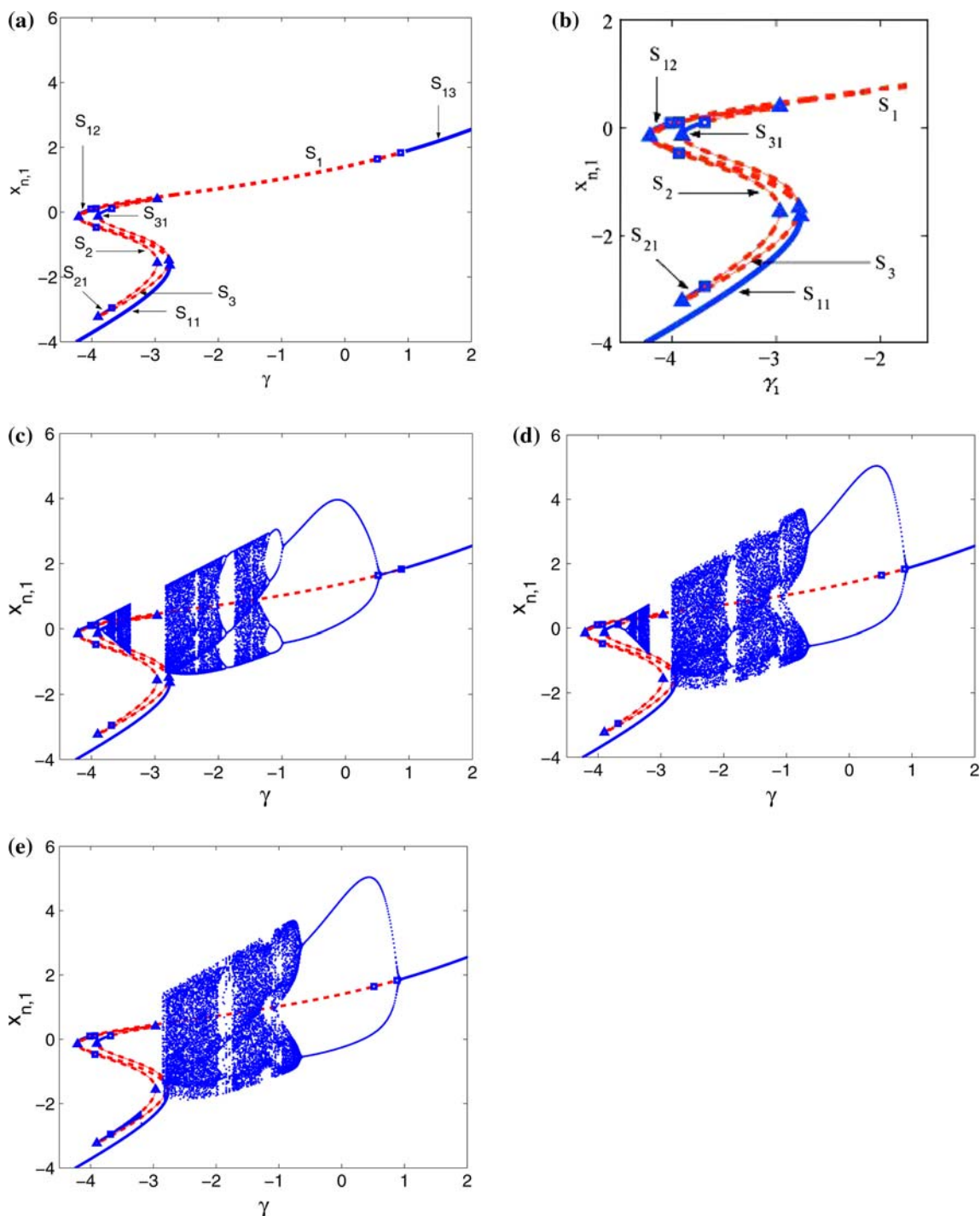


Fig. 2 These curves of fixed points and bifurcation diagrams correspond to the Eqs. (4) when $y_{n,1} = y_{n,2} = \gamma$, and $\varepsilon = 0.1$. **a** Three S-shaped curves of fixed points; **b** a blow-up of **a**; **c–e**

bifurcation diagrams are plotted with different initial conditions located on S_{12} , S_{31} , and S_{21} , respectively

conditions. For example, starting from off-diagonal fixed points on S_{31} and S_{21} , the subsequent chaotic oscillation is of a larger amplitude than that in Fig. 2c, and the boundaries of the chaotic oscillations are not much smoother than that in Fig. 2c. In view of these differences, we refer to the bursting resulting from the stable branches of on-diagonal

fixed points shown in Fig. 2c as the smooth bursting since ($x_{n,1} = x_{n,2}$), and the bursting resulting from the stable branches of off-diagonal fixed points shown in Fig. 2d–e as the non-smooth bursting since ($x_{n,1} \neq x_{n,2}$).

Due to the existence of an invariant manifold on S_{11} , the mechanism for bursting is similar to the one described by

Rulkov (2001) and de Vries (2001). That is, the mechanism leading to bursting still lies in the bistability region. In addition, there are multiple coexisting chaotic attractors depending on the different initial conditions. If the initial conditions are chosen from the multiple stable branches of off-diagonal fixed points of Eqs. (4), then the bifurcation diagrams of the fast subsystem Eq. (4) can predict the non-smooth *square-wave* bursting of the full system Eq. (1). If the initial conditions are chosen from the multiple stable branches of on-diagonal fixed points of Eqs. (4), then the bifurcation diagrams of the fast subsystem Eq. (4) can predict the regular smooth *square-wave* bursting of the full system Eq. (1).

Thus, the invariant manifold can play a very important role to study the dynamical behaviors of Eqs. (4). Due to the existence of an invariant manifold, much more complicated systems can be reduced into a comparatively simple low-dimensional subsystem by embedding them into the invariant manifold.

$$y_{n,1} \neq y_{n,2}$$

In this case, we suppose that $y_{n,1} = \gamma_1$ and $y_{n,2} = \gamma_2$, so that the corresponding fast subsystem is

$$\begin{aligned} x_{n+1,1} &= \frac{\alpha}{1 + x_{n,1}^2} + \gamma_1 + \varepsilon(x_{n,2} - x_{n,1}), \\ x_{n+1,2} &= \frac{\alpha}{1 + x_{n,2}^2} + \gamma_2 + \varepsilon(x_{n,1} - x_{n,2}). \end{aligned} \quad (5)$$

Note that Eqs. (5) are invariant (that is, are symmetric) under the transformation of $x_{n,1} \rightarrow x_{n,2}$ and $\gamma_1 \rightarrow \gamma_2$, and then the bifurcation diagram of $x_{n,1}$ versus γ_1 is the same as that of $x_{n,2}$ versus γ_2 .

For simplicity, we fix $\varepsilon = 0.1$ and $\gamma_2 = -2.7$, and we let γ_1 be a free parameter. The curves of fixed points of $x_{n,1}$ and $x_{n,2}$ versus the bifurcation parameter γ_1 are plotted together in a $(\gamma_1, x_{n,1} (x_{n,2}))$ plane shown in Fig. 3a. The purpose is to compare the similarity and differences between them, simultaneously. Here and afterwards, the thin lines stand for the curves of fixed points of $x_{n,1}$, while the thick lines stand for the curves of fixed points of $x_{n,2}$.

Note that on both the bottom curves of fixed points of $x_{n,1}$ and $x_{n,2}$, there coexist stable branches of fixed points, simultaneously. Moreover, the stability of both bottom stable branches of fixed points of $x_{n,1}$ and $x_{n,2}$ ends at the rightmost saddle-node bifurcation.

Two bifurcation diagrams are presented in Fig. 3b–c starting from different initial points located on the stable branches of fixed points of $x_{n,1}$ and $x_{n,2}$. In Fig. 3b, the initial point is chosen from the bottom stable branch of fixed points of $x_{n,1}$. When the iterates of $x_{n,1}$ are below the nullcline at $x_{n,1} = -1$, the slow variables $y_{n,1}$ will increase. Once the iterate attains the rightmost saddle-node bifurcation, the

silent phase ends and the active phase begins. When the iterates of $x_{n,1}$ exceed the nullcline $x_{n,1} = -1$, then the slow variable $y_{n,1}$ will decrease until γ_1 reaches the rightmost external crisis bifurcation. Subsequently, the iterate suddenly drops down onto the bottom stable branch of fixed points of $x_{n,1}$. Thus, a periodic transition between the silent phase and the active phase occurs, which corresponds to the so-called *square-wave* bursting.

Concerning the bifurcation diagram of $x_{n,2}$ versus γ_1 shown in Fig. 3c, the basic mechanism leading to bursting is similar to the one discussed above. However, it is necessary to point out that the transition between the silent phase and the active phase for both neurons are almost synchronized. This result can be seen clearly if we plot the aforementioned two bifurcation diagrams together as shown in Fig. 3d. In addition, seen from both Fig. 3b–d, there exist some transient periodic windows around $\gamma_1 = -4$. This is because the stability of the fixed points on the both upper branches shown in Fig. 3b–c changes at a Hopf bifurcations (denoted by squares). After the Hopf bifurcation, a route since the period-2 cycles to period-4 cycles, period-8 cycles, ..., and even period- n cycles or transient chaotic windows can be observed.

Thus, these results demonstrate that if we use two different bifurcation parameters to study the dynamics of a two-dimensional fast subsystem, then the fast subsystem is coexisting multiple coexisting synchronized attractors, which is useful to explain the in-phase synchronization of *square-wave* bursting of the full system Eq. (1).

Inhibitory electrical coupling

When the electrical coupling is inhibitory, the wave forms shown in Fig. 1c–d show that the two slow variables $y_{n,1}$ and $y_{n,2}$ are totally different even if the electrical coupling strength ε is small enough. Thus, in this section, the two different slow variables can only be treated as two different bifurcation parameters. We suppose that $y_{n,1} = \gamma_1$ and $y_{n,2} = \gamma_2$, and we fix $\varepsilon = -0.1$ and $\gamma_2 = -2.7$, while γ_1 is a free parameter.

The detailed curves of fixed points for $x_{n,1}$ and $x_{n,2}$ versus γ_1 are plotted together in Fig. 4a. There still coexist multiple stable branches of fixed points in this case. For example, concerning the curve of fixed points of $x_{n,1}$, there coexist two stable branches S_{11} and S_{12} . Concerning the curve of fixed points of $x_{n,2}$, there coexist three stable branches S_{21} , S_{22} , and S_{23} . But, in this case, there is no longer bistability.

Next, two different bifurcation diagrams corresponding to the first neuron and the second neuron, are plotted simultaneously. In Fig. 4b, once an initial point is chosen on S_{11} , the iterates of $x_{n,1}$ will undergo a two-period circle, four-period

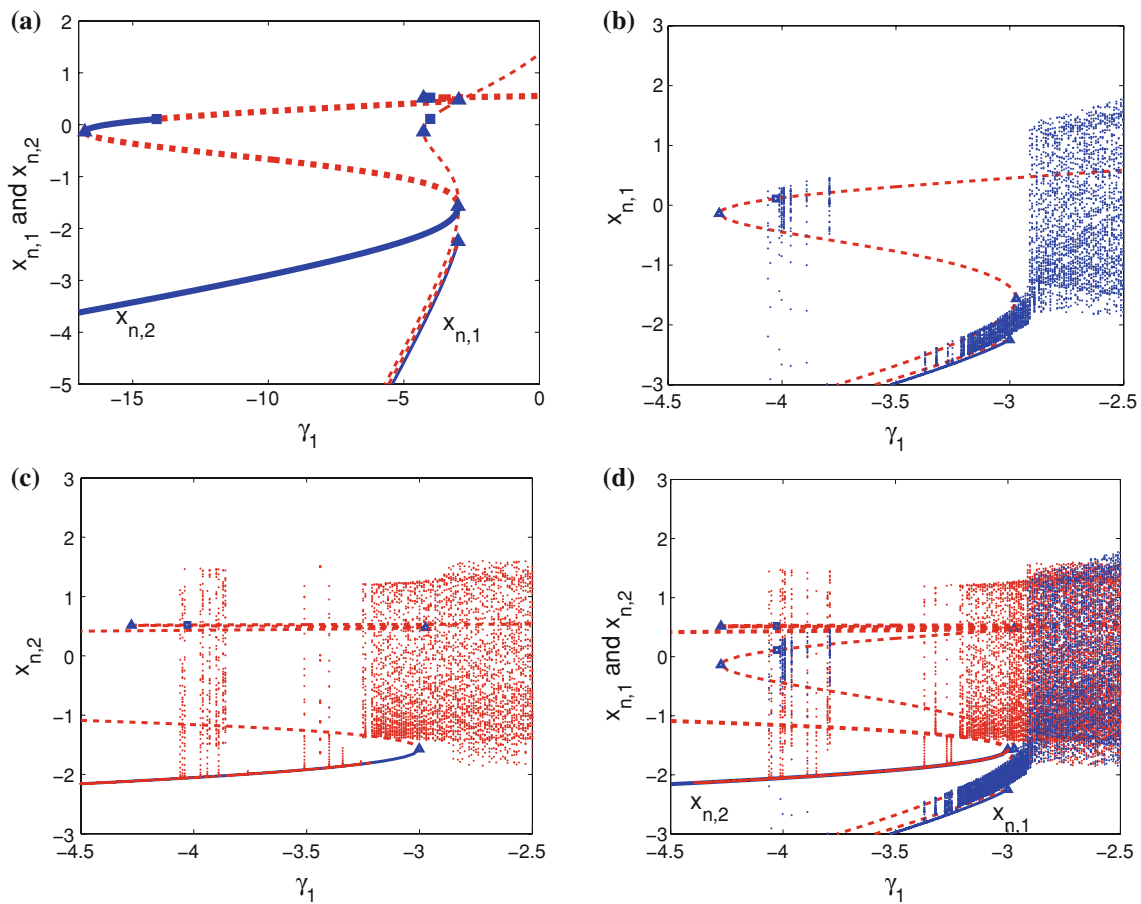


Fig. 3 These curves of fixed points and bifurcation diagrams correspond to the Eqs. (5) when $y_{n,1} = \gamma_1$, $y_{n,2} = \gamma_2$, $\varepsilon = 0.1$, and $\gamma_2 = -2.7$. **a** Curves of fixed points; **b–c** bifurcation diagrams with

circle, ..., and then the chaotic motion. When γ_1 reaches the leftmost external crisis bifurcation value at -3.582 , the iterate suddenly drops down onto the bottom unstable branch of fixed points of $x_{n,1}$. Then the iterates drop down onto the bottom chaotic attractor with small amplitude. That is to say, when $-3.582 \leq \gamma_1 \leq -3.0018$, seen from Fig. 4b, there exist a chaotic oscillation A_{11} with a comparatively small amplitude, here the parameter value of γ_1 at -3.0018 corresponds to the rightmost external crisis bifurcation. After the rightmost external crisis bifurcation, the iterate suddenly jumps up and a subsequent chaotic oscillation A_{12} occurs with a comparatively large amplitude.

Thus, the occurrence of chaotic attractor A_{11} can be predicted by the rightmost and the leftmost external crisis bifurcation values, while the second chaotic attractor A_{12} can be predicted by the leftmost external crisis bifurcation and the leftmost saddle-node bifurcation. Of course, as pointed out by Rulkov (2001) and de Vries (2001), because the occurrence of the attractor surrounding the unstable fixed points is chaotic when the bifurcation parameter γ_1 is near the external crisis bifurcation. The actual transition from the active to the silent phase can be delayed.

different initial conditions are plotted from the bottom stable branches of fixed points of x_1 and x_2 , respectively; **d** bifurcation diagrams of x_1 and x_2 are plotted together in the same figure

Because the position of the bottom chaotic oscillation A_{11} is always below the nullcline at $x_{n,1} = -1$, the slow variable $y_{n,1}$ is increasing. As what concerns the upper chaotic oscillation A_{12} , when the iterate of $x_{n,1}$ exceeds the nullcline at $x_{n,1} = -1$, the slow variable $y_{n,1}$ is decreasing. Therefore, once the chaotic oscillation A_{12} occurs, the iterate of $x_{n,1}$ will return to the bottom chaotic oscillation A_{11} . If the transient process of iteration is removed, then a kind of special transition in the order of $A_{11} \rightarrow A_{12} \rightarrow A_{11}$ occurs between the two chaotic oscillations A_{11} and A_{12} in a periodic fashion.

The mechanism described above can also explain the occurrence of *elliptic-like* bursting of the second neuron. However, in contrast to the order of *elliptic-like* bursting of the first neuron, the transition between the other two chaotic oscillations is in the order of $A_{21} \rightarrow A_{22} \rightarrow A_{21}$. If we plotted the above two bifurcation diagrams together, seen from Fig. 4d, when the first neuron produces the chaotic oscillation A_{11} with a small amplitude, the second neuron produces the chaotic oscillation A_{21} with a large amplitude; while when the first neuron produces the chaotic oscillation A_{12} with a large amplitude, the second neuron produces the

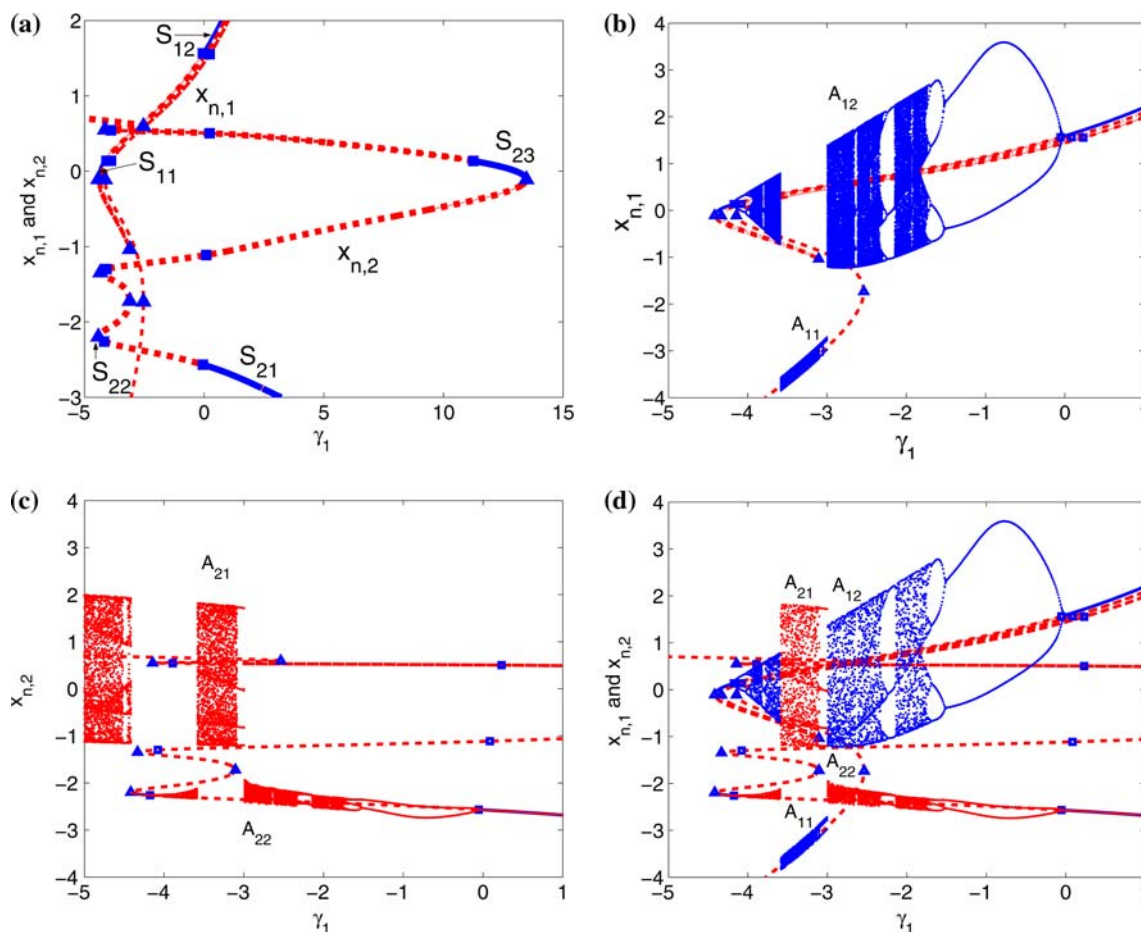


Fig. 4 These curves of fixed points and bifurcation diagrams correspond to Eqs. (5) when $y_{n,1} = \gamma_1$, $y_{n,2} = \gamma_2$, $\varepsilon = -0.1$, and $\gamma_2 = -2.7$. **a** Curves of fixed points; **b–c** bifurcation diagrams with

different initial conditions are plotted from the bottom stable branches of fixed points of x_1 and x_2 , respectively; **d** bifurcation diagrams of x_1 and x_2 are plotted together in the same figure

chaotic oscillation A_{22} with a small amplitude. Thus, the synchronized pattern between the first neuron and the second neuron is always in the state of antiphase.

Conclusion and discussion

In this paper, in view of the different consequences of considering excitatory or inhibitory electrical synaptic couplings, we have thoroughly analyzed the generation and synchronization of bursts of a network composed of two identical Rulkov map-based neurons. The emphasis of this paper is placed on the analysis of the fast–slow dynamics for a two-dimensional fast subsystem by either treating the two slow variables as a single bifurcation or two different bifurcation parameters, respectively.

Our results show that when the electrical synaptic coupling is excitatory, the invariant manifold of on-diagonal fixed points and the stability of the coexisting multiple stable branches of the off-diagonal fixed points can explain

and predict the generation of the in-phase and antiphase synchronization.

In contrast to this previous case, when the electrical coupling is inhibitory, the fast subsystem includes two different slow variables no matter how small the coupling strength is. In this case, the dynamical behaviors of the fast subsystem of the full system can be well predicted by using two different bifurcation parameters. By using this method, we obtain a mechanism for the occurrence of *elliptic-like* bursting, which is due to the interaction between two pair of chaotic attractors with different amplitudes. Furthermore, the generation of antiphase synchronization of networks lies in the different switching orders between two pairs of chaotic attractors of the first neuron and the second neuron.

The result obtained in this paper demonstrates that, if a two-dimensional fast subsystem is simplified into a one-dimensional fast subsystem after treating the two slow variables as a single bifurcation parameter, this simplification is only suitable for some specific coupling forms. While when the inhibitory synapses are considered, our analysis

shows that, even for a comparatively simple map-based network represented in this paper, the two slow variables can not be treated by using a single bifurcation parameter. Otherwise, some important information could be missed or even fail to predict the bursting oscillations. The results shown in this paper strongly suggest, as a consequence, that much attention should be paid on the different slow variables of neuron networks when bifurcation analysis and geometric singular perturbation method are used.

Acknowledgments This work is supported by the Program of Mobility of Foreign Researchers by the State Secretary of Universities and Research of the Spanish Ministry of Education and Science under project number SB2004-002 and the Grant from Chinese Natural Science Foundation under project number 10771012 (H. Cao), and by the Spanish Ministry of Education and Science under project number FIS2006-08525. H.Cao acknowledges the warm hospitality received at Universidad Rey Juan Carlos where this work was carried out.

References

- Best J, Borisyuk A, Rubin J, Terman D, Wechselberger M (2005) The dynamic range of bursting in a model respiratory pacemaker network. *SIAM J Appl Dyn Syst* 4:1107–1139
- Cao HJ, Ibarz B, Tanaka G, Sanjuán MAF (2007) The effect of asymmetry on generation and synchronization of bursts. *Phys Rev E* (submitted)
- Casado JM (2003) Transient activation in a network of coupled map neurons. *Phys Rev Lett* 91:20
- Casado JM, Ibarz B, Sanjuan MAF (2004) Winnerless competition in networks of coupled neurons. *Modern Phys Lett B* 18:1347
- Chialvo DR (1995) Generic excitable dynamics on a two-dimensional map. *Chaos Solitons Fractals* 5:461
- de Vries G (2001) Bursting as an emergent phenomenon in coupled chaotic maps. *Phys Rev E* 64:051914-1
- Elson RC, Selverston AI, Huerta R, Rulkov NF, Rabinovich MI, Abarbanel HDI (1998) Synchronous behavior of two coupled biological neurons. *Phys Rev Lett* 81:5692
- Gerstner W, Kistler WM (1999) *Spiking neuron models*. Cambridge University press, Cambridge
- Ibarz B, Tanaka G, Sanjuán MAF, Aihara K (2007a) Sensitivity versus resonance in two-dimensional spiking-bursting neuron models. *Phys Rev E* 75:041902
- Ibarz B, Cao HJ, Sanjuán MAF (2007b) Map-based neuron networks. In: Garrido PL, Marro J (eds) 9th Granada Seminar on computational and statistical physics, AIP Proceedings, 887. Melville, New York, p 69
- Ibarz B, Casado JM, Sanjuán MAF (2007c) Patterns in inhibitory networks of simple map neurons. *Phys Rev E* 75:041911
- Izhikevich EM (2000) Neural excitability, spiking and bursting. *Int J Bifurcat Chaos* 10:1171
- Izhikevich EM (2007) *Dynamical systems in neuroscience: the geometry of excitability and bursting*. The MIT press, Cambridge
- Nozawa H (1992) A neural network model as a globally coupled map and applications based on chaos. *Chaos* 2:377
- Rinzel J (1987) *Mathematical topics in population biology, morphogenesis, and neuroscience*. Springer, New York
- Rulkov NF (2001) Regularization of synchronized chaotic bursts. *Phys Rev Lett* 86:183
- Rulkov NF, Timofeev I, Bazhenov M (2004) Oscillations in large-scale cortical networks: map-based model. *J Comput Neurosci* 17:203
- Shilnikov AL, Rulkov NF (2004) Subthreshold oscillations in a map-based neuron model. *Phys Lett A* 328:177
- Tanaka G, Ibarz B, Sanjuán MAF, Aihara K (2006) Synchronization and propagation of bursts in a ring of coupled map neurons. *Chaos* 16:013113
- Sherman A (1996) Contributions of modeling to understanding stimulus secretion coupling in pancreatic β -cells. *Am J Physiol Endocrinol Metab* 271:E362–E372